Si(111) step fluctuations at high temperature: Anomalous step-step repulsion

Saul D. Cohen,[1,*] Robert D. Schroll,[1] T. L. Einstein,[1] J.-J. Métois,[2] Hailu Gebremariam,[1]
Howard L. Richards,[1,†] and Ellen D. Williams[1]
[1]*Department of Physics, University of Maryland, College Park, Maryland 20742-4111*
[2]*CRMC2-CNRS, Campus Luminy, Case 913, F-13288 Marseille Cedex 9, France*
(Received 18 March 2002; revised manuscript received 28 June 2002; published 12 September 2002)

Using reflection electron microscopy we examine the step fluctuations of Si(111) at 1100 °C. Evaporation is compensated by a replenishing flux. The step fluctuation behavior is qualitatively similar to that at 900 °C (where sublimation is negligible), with unexplained quantitative differences. We focus on the three parameters of the step continuum model of vicinals. The step stiffness scales with an increase in T from 900 °C as predicted by an appropriate lattice model. The kinetic coefficient is larger than scaling of the parameters from 900 °C would predict. The step-step correlations are assessed in traditional and novel ways; step repulsions are at least 6 times as strong as predicted from lower temperatures, suggesting nonequilibrium effects probably due to electromigration.

DOI: 10.1103/PhysRevB.66.115310 PACS number(s): 05.40.−a, 05.70.Np, 68.35.Md, 68.37.−d

I. INTRODUCTION

Step fluctuations of vicinal Si(111) have attracted active experimental interest for nearly a decade. Silicon is chosen not just for its industrial importance but also because its low defect density implies that the fluctuations will be relatively unimpeded by pinning sites. Unlike the more popular (100) surface, the (111) surface does not require distinguishing between s_A and s_B steps.

A primary goal in studying step fluctuations is to determine the dominant mechanism of atomic mass transport that underlies the step motion. When the atoms are confined to the surface, there are three long-known[1] limiting regimes for isolated steps: (1) periphery diffusion (PD), dominated by adatom motion along the step edge; (2) terrace diffusion (TD), governed by the terrace diffusion constant D; and (3) two-dimensional (2D) evaporation and condensation (EC) or attachment and detachment, in which the rate-limiting step is detachment from the step edge—controlled by the kinetic coefficient ν—with uniform adatom concentration c. In the continuum step model,[2] which has been remarkably successful in accounting for a broad range of morphological-evolution phenomena,[2,3] the behavior of the step is characterized in terms of parameters on a scale much greater than atomic: specifically, one seeks the step stiffness, the strength of the interactions between steps, and a third parameter characterizing the dynamics, essentially ν. The first and third can be gleaned from the step fluctuations of individual steps and the second from the distribution of their spacings. As the characteristic length[4] $d \equiv D/\nu$ varies from the TD limit of 0 to the EC limit of ∞, one finds intermediate behavior, but the characteristic exponent z changes over a narrow range of d.[5]

Step fluctuations of vicinal Si(111) have been extensively studied in the narrow thermal range above the $7\times7-$"1×1" phase transition ($\sim$860 °C), where steps are very mobile, but sublimation is insignificant. In a capillary-wave analysis of reflection electron microscope (REM) data[6,7] taken at 900 °C, Bartelt *et al.*[8] showed that the fluctuations were not due to PD and that, in the EC framework, $\sim10^6$ attachment or detachment events per second occurred at step sites. The EC picture also underlies a quantitative theory of current-induced step bunching on Si(111).[9] However, diffusion between steps may also contribute significantly;[10] in finite-size limited TD, fluctuations with lateral size q^{-1} have the same decay time $\propto q^{-2}$ as in EC.[5,11] In a LEEM (low-energy electron microscope) study of the decay of islands at 814–877 °C, both the temporal behavior and nonuniform accumulation of atoms on steps had the signatures of TD.[12]

Here we consider slightly vicinal Si(111) at much higher temperature $T=1100$ °C, at which there is a sizable sublimation $\sim$0.015 BL/s [1 bilayer (BL) $\equiv 1.56\times10^{19}$ atoms/m^2]. Since the mean step separation $\langle l\rangle$ was $\sim$250 nm, this evaporation amounts to a net loss per step site of 11 atoms/s. In order to replenish this loss, a second Si wafer is placed close by, $\sim$100 μm away. This "source" wafer is heated independently to a T slightly higher than the "sample" wafer to ensure that there is no systematic motion—advancement or retreat—of the steps on the sample. The heating is by dc electric current, in the downstairs, nonbunching direction. (The twin-crystal sample holder has previously been described in detail.[13] A similar arrangement was used earlier by Latyshev *et al.*[14] to study this surface, albeit with attention to the initial stages of homoepitaxy.) Only with a grazing probe like REM is such an arrangement feasible. (To study rapid fluctuations, REM is preferable to scanning probes, which may miss significant motion between scans.)

The Si system is in a steady state, by which we mean that there is no overall change in mass, i.e., no net advancement or retraction of the steps. The question of whether the system is in equilibrium is more subtle. In the experiments around 900 °C, below significant sublimation, the system was in 2D equilibrium, with surface mass strictly conserved. In the present case, atoms adsorb onto and desorb from the surface. Although the average rates are the same, there are fluctuations in mass in addition to the fluctuations of the steps produced by 2D attachment and detachment. Since the latter events are orders of magnitude more frequent, one would expect little change from equilibrium. Also, we noted above that the source crystal must be at a slightly higher temperature than the sample in order to compensate for atoms lost to

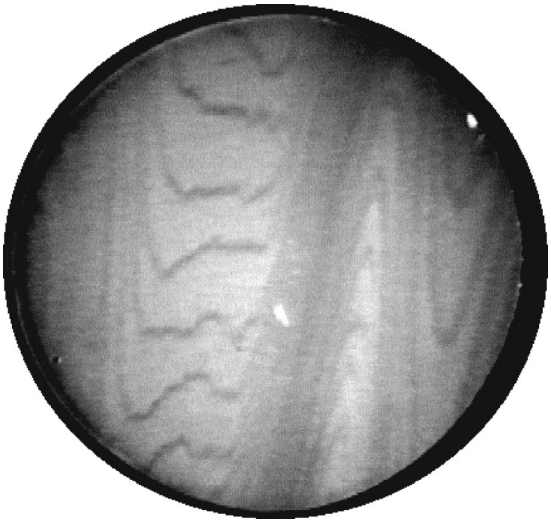

FIG. 1. Photo of a typical REM image frame. The $\hat{x}$ is determined by the nearly vertical line connecting the sequence of sharp crests of the steps (dark curves) of the near right side of the image. There is a 35-fold compression along the perpendicular, nearly horizontal $\hat{y}$ axis. Only data from the nearly straight part of the steps nearly parallel to $\hat{y}$ were analyzed.

the background. However, the major reason that the system is not in equilibrium is that the dc heating current produces electromigration. Thus, there is a net driving force on the steps, in this case in the unbunching direction.

In the next section, we mention some experimental details. The following two sections consider spatial correlation functions of single steps and sets of steps to extract information about about the step stiffness and the step-step repulsion strength, respectively. The latter section describes a new way of finding this repulsion strength using the step-step correlation function. The following section discusses temporal correlations, and the final section offers a brief conclusion.

II. EXPERIMENT

The experiment was performed in Marseilles on the REM apparatus described in Ref. 6. Frames were recorded in SECAM format (but at 24 frames per second) with a Sony video camera from a TV screen using helical scanning with 330-line resolution. A sample frame is shown in Fig. 1. Several challenges impede quantitative analysis of this data. The foreshortening by a factor of nearly 35:1 along an axis close to the mean step direction (called $\hat{y}$ in ''Maryland notation'') is a well-known factor that makes precise alignment of the step direction difficult. (The 400-pixel diameter corresponds to 1.8 μm and 62 μm in the $\hat{x}$ and $\hat{y}$ directions, respectively.)

The difficult implementation of the double-crystal configuration created instabilities in the images, e.g., sporadic jumps between images due to electrostatic discharges, which created significant challenges in studying dynamics. Furthermore, steps appeared and disappeared as the video elapsed, making it hard to reliably compute terrace-width distributions between neighboring steps or to track the evolution of

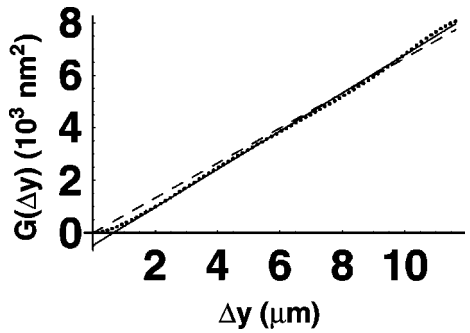

FIG. 2. Plot of $G(\Delta y) \equiv \langle [x(y+\Delta y)-x(y)]^2 \rangle$ vs Δy for 5000 frames of data. The straight lines are linear fits. (See text.) The slope is $k_B T/\tilde{\beta}$.

points on a step. We analyzed a range of 5000 frames out of 12 000 for which these effects were least problematic. The application of new, alternative analysis approaches allowed us to assess the effects of image instabilities.

III. STEP STIFFNESS

Arguably the most reliable way to extract the step stiffness $\tilde{\beta}$ is to view a step kink as a ''pace'' of a random walker along $\hat{x}$ as ''time'' evolves along $\hat{y}$; then $\tilde{\beta}$ is proportional to the inverse of the diffusivity,

$$\tilde{\beta} = k_B T \Delta y / G(\Delta y), \tag{1}$$

where $G(\Delta y)$ is the spatial correlation function at constant of a ''snapshot'' (i.e., at constant physical time):

$$G(\Delta y) \equiv \langle [x(y+\Delta y)-x(y)]^2 \rangle. \tag{2}$$

The mean-square deviation is indeed quite linear in displacement along $\hat{y}$ (cf. Fig. 2); from the slope we estimate $\tilde{\beta} = 16.3 \pm 1.8$ meV/Å. This value allows for a small offset at the origin. Without it, our fit is notably poorer and $\tilde{\beta}$ nearly 2 meV/Å larger. This offset seemingly comes from a slight misalignment of the calibration axes.

Alternatively, one can measure the mean-square wandering of the entire step. From equipartition comes the expectation that $\tilde{\beta}$ can be deduced from the mean-square deviation $\langle x^2 \rangle$ (Ref. 11):

$$\langle x^2 \rangle = k_B T L / 12 \tilde{\beta} \quad \text{(free ends)}, \tag{3}$$

where L is the length of the step (along $\hat{y}$) over which $\langle x^2 \rangle$ is found. [For fixed ends in the model of the step as a vibrating string, 6 replaces 12 in the denominator of Eq. (3).] In this way, REM measurements[6] led to[11,15] the estimate $\tilde{\beta} \approx 46$ meV/Å at 900 °C. In a similar analysis at 1100 °C (for which modeling with free boundary conditions was more appropriate) produces $\tilde{\beta} \approx 12$ meV/Å, about 3/4 the value from the diffusivity analysis. Also, the fit is considerably noisier, particularly when step lengths are greater than 75 pixels (so ~ 12 μm).

This value is about half the $\tilde{\beta}$ of 30 meV/Å obtained at 900 °C,[8] chosen as a calibration standard.[16] If $\tilde{\beta}(T) \propto \exp(\epsilon/k_BT)$,[17] where ϵ is the kink energy, then $\tilde{\beta}(1100\,^\circ\mathrm{C})$ should be $\sim 70\%$ of $\tilde{\beta}(900\,^\circ\mathrm{C})$. A more accurate expression[16] taking into account the geometry of Si(111) reduces this ratio to $\sim 1/2$,[18] as in the experiment.

IV. STEP REPULSION STRENGTH

The second parameter of the step continuum model describes the strength A of the step-step repulsion. This repulsion per unit length along the step, which is generally assumed to be elastic in origin and dipolar in nature, has the form A/l^2, where l is the step spacing. (In many formulations,[2] the second parameter is called g and then includes the entropic contribution to the step repulsion, which also goes like $1/l^2$—but in a way more complicated than simple addition.) To estimate A one typically analyzes the terrace-width distribution (TWD). Some of us have argued repeatedly[19–23] that the TWD can be well described by the ''generalized Wigner distribution''

$$P_\varrho(s) = a_\varrho s^\varrho \exp(-b_\varrho s^2), \tag{4}$$

where $s \equiv l/\langle l \rangle$, while a_ϱ and b_ϱ are [ϱ-dependent] constants that assure normalization and unit mean, respectively.[19,22] The value of ϱ is obtained by optimizing the fit of Eq. (4) to the data.[24] From ϱ one can quickly obtain A (Ref. 25):

$$\tilde{A} = \varrho(\varrho - 2)/4 \quad \text{and} \quad A = \tilde{A}(k_BT)^2/\tilde{\beta}. \tag{5}$$

Alternatively, from the measured[26] variance σ^2 of the TWD, one can obtain $\tilde{A}$ using the relation[21]

$$\tilde{A} \simeq \frac{1}{16}\left[\frac{1}{(\sigma^2)^2} - \frac{7}{\sigma^2} + \frac{27}{4} + \frac{35}{6}\sigma^2\right]. \tag{6}$$

Using Eq. (4) we deduced $\varrho \approx 5$, so that $\tilde{A} \approx 4$.

However, this estimate might be biased toward too broad a distribution, i.e., too weak an interaction, due to the occasional but pervasive disappearance (and reappearance) of step images in the digitized frames. Fortunately, we can instead find $\tilde{A}$ by analyzing the step correlation function h,[22] i.e., the probability of finding another step a specified distance away, *regardless of how many steps might lie between them*. We write S for this separation divided by the mean step spacing: it is similar to s in its normalization, but the capital case provides a reminder that there can be intervening steps (particles), so that $h_\varrho(S)$ approaches the mean step density $\langle l \rangle^{-1}$ for large S, while $P_\varrho(s)$ vanishes monotonically in this limit. Since it is a two-particle correlation function, $h_\varrho(S)$ is generally easier for a theoretician to compute than the TWD $P_\varrho(s)$, which corresponds to a many-particle correlation function.[27]

Qualitatively, $h_\varrho(S)$ initially increases as S^ϱ, analogous to the s^ϱ behavior of $P_\varrho(s)$, since there are not likely to be intervening steps at separations much less than the mean. At each positive integer value of S, there is a peak of $h_\varrho(S)$. The envelope associated with these oscillations decreases monotonically with S, as for the pair correlations of a liquid, so that (as noted) $h_\varrho(S)$ eventually approaches the mean density. This behavior is exhibited by the relatively simple ''harmonic,'' lattice approximation[28–30]

$$\langle l \rangle h_\varrho(S) = \sum_{m \neq 0} (B_m \pi)^{1/2} \exp[-B_m (S-m)^2],$$

$$\frac{\pi^2 \varrho}{4B_m} = \gamma + \ln(2\pi m) - \mathrm{ci}(2\pi m) = \sum_{j=1}^{\infty} (-1)^{j+1} \frac{(2\pi m)^{2j}}{2j(2j)!}, \tag{7}$$

where $\gamma \simeq 0.577$ is Euler's constant and ci is the cosine integral.[31] Note that B_m is proportional to ϱ, so that peaks become sharper and higher with increasing repulsion. Also, B_m/ϱ decreases rather gradually (but somewhat faster than exponentially) with increasing m: e.g., $B_1 \doteq 1.012\varrho$, $B_3 \doteq 0.702\varrho$, $B_5 \doteq 0.613\varrho$, $B_{10} \doteq 0.523\varrho$, $B_{20} \doteq 0.456\varrho$, and $B_{40} \doteq 0.404\varrho$. While useful for many applications,[28–30] this approximation for $h_\varrho(S)$ proved inadequate for deducing ϱ from data.

As just noted, it is easier to compute $h_\varrho(S)$ than $P_\varrho(s)$. In fact, there is an exact, albeit unwieldy (and not concisely expressible), solution[28] for $h_\varrho(S)$ at even-integer values of ϱ.[32] (Furthermore, numerical implementation of this solution becomes somewhat problematical for S much larger than 3.) It is more convenient to use a recently formulated asymptotic expression[33]

$$\langle l \rangle h_\varrho(S) \sim -\frac{1}{\pi^2 \varrho S^2} + 2\sum_{j=1}^{\infty} \frac{d_j^2(\varrho)}{(2\pi S)^{4j^2/\varrho}} \cos(2\pi j S),$$

$$d_j(\varrho) = \Gamma\left(1 + \frac{2j}{\varrho}\right) \prod_{m=1}^{j-1} \left(\frac{2m}{\pi\varrho}\right) \sin\left(\frac{2\pi m}{\varrho}\right) \Gamma^2\left(\frac{2m}{\varrho}\right), \tag{8}$$

which provides a good description for $S > 1/2$; it can be patched onto $a_\varrho S^\varrho$ for $S \leqslant 1/2$. All these expressions assume an infinite system (or a ring). Since there are only about half a dozen steps in our frames (cf. Fig. 1), the experimental $h_\varrho(S)$ will vanish for large S. The simplest form for the consequent envelope of $h_\varrho(S)$ decays linearly, vanishing for the length of the frame in $\hat{x}$. With this assumption we found a decent description of the experimental pair correlations for $\tilde{A} \approx 6 \pm 1$ (cf. Fig. 3), somewhat but not dramatically larger than deduced from the TWD. [Note also a fit of the first peak of $h_\varrho(S)$ in Fig. 3 yields $\tilde{A} \approx 4.8$.]

For comparison, at 900 °C, $\tilde{A}$ is 1.7.[15,34] Since $\tilde{A}$ is expected to *decrease* with increasing T [cf. Eq. (5); A is normally insensitive to T], our value for $\tilde{A}$ is strikingly large. Since $(k_BT)^2/\tilde{\beta}$ is 2.74 times as large at 1100 °C, A increases by at least a factor of ~ 6 and perhaps up to ~ 10. This remarkable finding says that the fluctuations in step spacings are strongly *suppressed* compared to the extrapolated equilibrium value at 1100 °C. Such narrowing of the terrace distribution is known to occur in step-flow growth[35] or etching, even though our coverage is essentially constant. In other words, this steady-state situation may give measur-

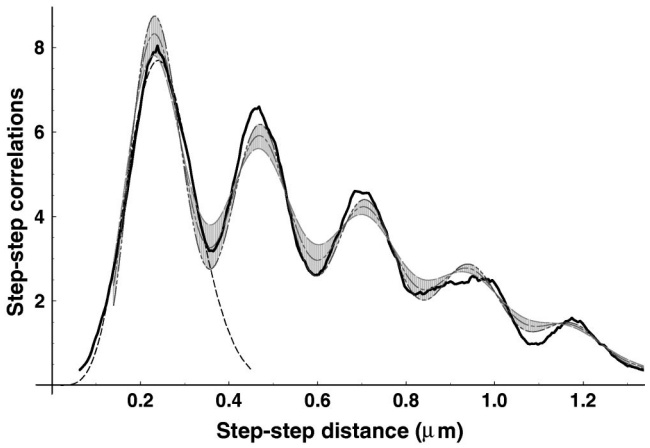

FIG. 3. Pair (step-step) correlation function, in arbitrary units, showing the data (thick solid curve) as well as theoretical expectations based on Eq. (9) for $h_\varrho(S)$ with a linear envelope due to the small number of steps in experimental frames: the gray-shaded region is bounded by $\varrho=5$ (dashed line, with smaller oscillations) and $\varrho=7$ (dash–double-dotted line with larger oscillations). In the middle of the gray region, the dash-dotted curve is $\varrho=6$. The values $\varrho=5$, 6, and 7 correspond to $\tilde{A}\approx 4$, 6, and 9, respectively. The single-peaked short-dashed curve is a fit of Eq. (4) to the first peak, with $\varrho=4.8$, similar to $\varrho\approx 5$ from fitting the TWD.

ably different behavior than equilibrium behavior for three-dimensional evaporation and condensation. On the other hand, given the small rate of 3D events, one must question whether some other dramatic change in the surface—but not the steps—has occurred between 900 °C and 1100 °C. Such changes are known to occur in electromigration on Si(111): behavior between 1000 °C and 1180 °C is distinctly different from behavior in lower- (and in higher-) T regimes.[36] Also noteworthy is the finding[37]—albeit at well over 100 °C above this experiment—that there is a sizable increase in both $\tilde{\beta}$ and $\tilde{A}$, which has been interpreted as due to changes in step permeability.

Monte Carlo simulations[35] show that growth alters TWD's considerably. Thus, we compare the physical parameters for Si(111) with those of a model of growth-induced narrowing of distributions. Associated with a deposition rate F is a meandering width[38] $(\Omega D c_{\rm eq} k_B T/2\tilde{\beta} d^2 F)^{1/4}\langle l\rangle^{1/4}$, where Ω is the atomic area and $c_{\rm eq}$ the equilibrium adatom concentration. It becomes controlling, i.e., smaller than the width attributed to elastic repulsions $\approx(8\tilde{A})^{-1/4}\langle l\rangle$, for large enough flux and d, viz., for $Fd^2>4\tilde{A}\Omega D c_{\rm eq} k_B T/\langle l\rangle^3\tilde{\beta}\approx 2\times 10^4\ {\rm s}^{-1}$. ($Dc_{\rm eq}\approx 2\times 10^{11}\ {\rm s}^{-1}$ is estimated below.) While arguably irrelevant to our steady state, we note that for the flux at 1100 °C *uncompensated* by desorption, this criterion becomes $d>400$ nm, which is consistent with results in an electromigration experiment on Si(111) at 930 °C.[39]

Such narrowing of the TWD ultimately comes from biased diffusion to ascending steps due to the Ehrlich-Schwoebel barrier.[4] Since electromigration produces a similar asymmetry,[40–42] it should have similar consequences, especially given recent arguments about universality in step bunching,[43] but there has been no detailed analysis of the reduction in meandering. Qualitatively, since bunching amounts to the effective $\tilde{A}$ becoming negative $(\tilde{A}<-1/4)$,[22,44] current in the opposite direction might well *increase* the effective value of $\tilde{A}$ considerably. (However, electromigration should have a minute effect on the stress dipole at steps, which underlies the actual A.) Since calculations of step effects in electromigration are now possible,[45] our findings will hopefully stimulate computational investigations to quantify these effects, as well as more systematic experiments to gauge the current dependence of the TWD width.

V. TEMPORAL CORRELATIONS

To determine whether the suppresssion of step wandering is correlated with any anomalous changes in the kinetic parameters, we evaluated the temporal correlations via a capillary-wave analysis.[8] By discrete Fourier transform along the step direction, one generates $x_q(t)$ from $x(y,t)$, choosing q as an integral multiple of $2\pi/N$, where N is a fixed number of pixels along the step, typically 64 in our analysis. The correlations of these Fourier components are expected to obey the relation[8]

$$G_q(\Delta t)\equiv\langle|x_q(t+\Delta t)-x_q(t)|^2\rangle=\frac{2k_BT/L}{\tilde{\beta}q^2+c}(1-e^{-\Delta t/\tau_q}). \tag{9}$$

While Eq. (9) dictates that $G_q(\Delta t)$ start at the origin, the data have a finite positive offset, reminiscent of that seen for ''frizzy'' steps in scanning tunneling microscopy (STM) experiments.[46–48] In that case, the offset comes from an inadequate scan rate, which allows unrecorded jumps of the step position between scans. The analogy is confirmed by the finding below that the characteristic times τ_q in Eq. (9) are comparable to the scan rate of the video camera. (The problem is confounded by the interleave nature of the scanning.) For the STM experiments, the offset is sometimes attributed to tip effects,[48] which are manifestly absent for REM. In the STM experiments, the offset is typically treated as a constant in the real-space, repeated-scan correlation function. Here the offset scales roughly like q^{-2}, thus of a compatible form.[49] From Eq. (9) we note that when c is negligible, one can collapse the results for various values of q onto a single curve by plotting $q^2G_q(\Delta t)$ as a function of $\Delta t/\tau_q\rightarrow q^2\Delta t$. While the horizontal scaling is only fair, the vertical scaling of the offset is obviously reproduced. (It is curious that data have not typically been subjected to such a scaling test.) With this caveat, we proceed to analyze the data as if there were no offset. (If we subtract the offset before analyzing the data,[46,47] the quality of the fits degrades severely and the deduced parameters are unreasonable.)

In Fig. 4 we show a graph of the denominator in Eq. (9), $\tilde{\beta}q^2+c$, plotted versus q. The fit to a quadratic is excellent, and the deduced coefficient $\tilde{\beta}$ is 12.6 ± 1.3 meV/Å with a miniscule value for c of $(-2.8\pm 0.7)\times 10^{-8}$ meV/Å^3. (The error bars are deduced by fitting different ranges of frames.)

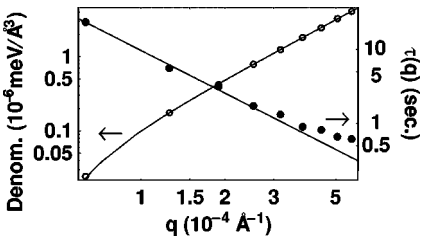

FIG. 4. Log-log plots, vs q, of $\tilde{\beta}q^2+c$ [i.e., the denominator in Eq. (9)] (left ordinate, circles), and of τ_q (right ordinate, dots). The solid lines show fits to the data. For the circles, this fit is to the quadratic $\tilde{\beta}q^2+c$. For the dots, it determines the dynamic exponent z from the ansatz $\tau_q \propto q^{-z}$.

From the fit to Eq. (9) we simultaneously extract estimates of τ_q, which is expected to scale like q^{-z}, where for an isolated step $z=2$, 3, and 4 for EC, TD, or PD, respectively;[2,46,50] the best-fit (shown in Fig. 4) value of z is 1.9 ± 0.2. While this value is consistent with EC behavior, we caution that $q\langle l\rangle \approx 1$ near the middle of the abscissa of Fig. 4, so in the middle of the crossover region from DSS (diffusion step to step, with $z=2$) to TD (with $z=3$) at large values.[5,11] Using $\tau_q = k_B T/\Gamma_a \tilde{\beta} q^2$ to gauge the ''step mobility'' Γ_a yields $(1.3\pm0.1)\times10^9$ Å^3/s. This value is about 20 times that found previously at 900 °C,[8] which corresponded to a time interval of order 10^{-6} s between 2D attachment or detachment events at a step site.[8] If instead we assume the DSS form[11] $\tau_q = k_B T \pi^2 \langle l\rangle/\tilde{\beta}\Omega^2 D c_{\rm eq} q^2$, then $D c_{\rm eq} \approx 2\times10^{11}$ s^{-1}, about 70 times the value at 900 °C. These increases in the rate parameters are substantially larger than the fivefold to ninefold fold increase that would have been expected for a simple activated rate with $E_a = 1$–1.5 eV. It seems highly unlikely that the large rates could be caused by the sublimation-deposition fluxes, which correspond to only ~10 step-edge events per second.

While often used, to distinguish between mass transport mechanisms, the time correlation function in real space:

$$G_x(\Delta t) = \langle [x(y,t+\Delta t) - x(y)]^2 \rangle_{y,t} = \sum_{q=-\infty}^{\infty} G_q(\Delta t), \tag{10}$$

proved particularly difficult to analyze. For small Δt, $G_x(\Delta t) \propto (\Delta t)^{1/z}$; in particular, in the EC limit, $G_x(\Delta t) \sim (2k_B T\Gamma_a/\pi\tilde{\beta})^{1/2}(\Delta t)^{1/2}$.

To contend with the above-noted vagaries of the data, the best of several schemes involved tracking individual pixels at step locations with an adjustable window in $\hat{x}$. If this window is much less than the step roughness (wandering), then the exponent is too small ($z^{-1} \sim 0.36$) because substantial deviations are lost. If much larger than the mean step separation, then steps get confused, and again the z^{-1} is too small (~ 0.25). Between these two extremes lies a broad ''plateau'' over which $z^{-1} \sim 0.6$. Furthermore, at large Δt a spurious hump appeared in $G_x(\Delta t)$. Restricting our analysis to smaller values of Δt, we determine $z^{-1} = 0.58 \pm 0.06$.

VI. CONCLUSION

In the step continuum model, a vicinal surface is described by the stiffness of its steps, the strength of their mutual repulsion, and the coefficient characterizing the rate-limiting mode of mass transport. The most appropriate test of the picture is whether the same set of parameters describes a broad range of phenomena at or near equilibrium. In the present study, we consider Si(111) at 1100 °C in steady state, i.e., with no net advancement or retreat of steps, and compare results for the three parameters with values extrapolated from equilibrium measurements at 900 °C. While the measured step stiffness is consistent with expectations from such an extrapolation, the apparent step repulsion is much stronger than expected, as is physically manifested in a narrowing of the TWD. This finding is an indication that the system is far from equilibrium even if at constant coverage, i.e., with mass conserved on average. The most probable source of the unexpectedly large deduced value of the step repulsion is electromigration effects arising from the heating current. Obviously it would be desirable to check this conclusion by performing a similar experiment at 1100 °C with a different heating mechanism, even though a number of technical problems make this a daunting challenge. (Reversing the direction of the heating current in REM causes a small jump in the image, so the rapid-ac heating results in an unacceptably blurred image.) Finally, the dynamics seem consistent with the evaporation-condensation mechanism, but the increase in the kinetic parameters between 900 and 1100 °C is about 5 times larger than would be predicted for accepted values for the activation energy.

ACKNOWLEDGMENTS

Work at Maryland was supported by our MRSEC (NSF-DMR 00-80008). R.D.S. benefited from support from the University of Maryland. Some recent work of S.D.C. and T.L.E. has been partially supported by NSF Grant No. EEC-0085604. T.L.E. and J.J.M. are grateful for the hospitality of M. Uwaha and Nagoya University, as well as partial support from JSPS Research for the Future Program in the Area of Atomic Scale Surface and Interface Dynamics. We thank Bhaskar L. Khubchandani and Dr. Zóltan Toroczkai for their help in the initial phases of processing the data and Dr. Igor Lyubinetsky for fruitful suggestions.

*Present address: Dept. of Physics, Columbia University, New York, NY 10027.
†Permanent address: Dept. of Physics, Texas A&M University–Commerce, Commerce, TX 75429-3011.

[1] W.W. Mullins, J. Appl. Phys. **28**, 333 (1957); **36**, 77 (1959).
[2] H.-C. Jeong and E.D. Williams, Surf. Sci. Rep. **34**, 171 (1999).
[3] A. Ichimiya, K. Hayashi, E.D. Williams, T.L. Einstein, M. Uwaha, and K. Watanabe, Phys. Rev. Lett. **84**, 3662 (2000).
[4] A. Pimpinelli and J. Villain, *Physics of Crystal Growth* (Cambridge University Press, Cambridge, England, 1998).

[5] S.V. Khare and T.L. Einstein, Phys. Rev. B **57**, 4782 (1998), which uses the notation $a_q \equiv |q|d$.
[6] C. Alfonso, J.M. Bermond, J.C. Heyraud, and J.J. Métois, Surf. Sci. **262**, 371 (1992).
[7] Z. L. Wang, *Reflection Electron Microscopy and Spectroscopy for Surface Analysis* (Cambridge University Press, Cambridge, England, 1996).
[8] N.C. Bartelt, J.L. Goldberg, T.L. Einstein, Ellen D. Williams, J.C. Heyraud, and J.J. Métois, Phys. Rev. B **48**, 15 453 (1993).
[9] D.-J. Liu and J.D. Weeks, Phys. Rev. B **57**, 14 891 (1998).
[10] T. Ihle, C. Misbah, and O. Pierre-Louis, Phys. Rev. B **58**, 2289 (1998).
[11] A. Pimpinelli, J. Villain, D.E. Wolf, J.J. Métois, J.C. Heyraud, I. Elkinani, and G. Uimin, Surf. Sci. **295**, 143 (1993).
[12] H. Hibino, C.-W. Hu, T. Ogino, and I.S.T. Tsong, Phys. Rev. B **63**, 245402 (2001), which provides a thorough discussion of work subsequent to Ref. 8.
[13] J.C. Heyraud, J.J. Métois, and J.M. Bermond, Surf. Sci. **425**, 48 (1999).
[14] A.V. Latyshev, A.L. Aseev, A.B. Krasilnikov, and S.I. Stenin, Phys. Status Solidi A **113**, 421 (1989).
[15] J.M. Bermond, J.J. Métois, J.C. Heyraud, and F. Floret, Surf. Sci. **416**, 430 (1998).
[16] N. Akutsu and Y. Akutsu, J. Phys.: Condens. Matter **11**, 6635 (1999).
[17] N.C. Bartelt, T.L. Einstein, and E.D. Williams, Surf. Sci. **276**, 308 (1992).
[18] From Fig. 6 of Ref. 16 we find this ratio to be 44% and 51% for the $(2\bar{1}1)$ and $(\bar{2}11)$ steps, respectively. Although Ref. 8 did not distinguish between $(2\bar{1}1)$ and $(\bar{2}11)$ steps, Fig. 6 was calibrated by assuming that Ref. 8 studied $(2\bar{1}1)$.
[19] T.L. Einstein and O. Pierre-Louis, Surf. Sci. **424**, L299 (1999).
[20] M. Giesen and T.L. Einstein, Surf. Sci. **449**, 191 (2000).
[21] H.L. Richards, S.D. Cohen, T.L. Einstein, and M. Giesen, Surf. Sci. **453**, 59 (2000).
[22] T.L. Einstein, H.L. Richards, S.D. Cohen, and O. Pierre-Louis, Surf. Sci. **493**, 460 (2001).
[23] T.L. Einstein, J. Jpn. Assoc. Cryst. Growth **29**, 20 (2002).
[24] In studying physical (in contrast to Monte Carlo) data, it is usually best to perform a two-parameter fit in terms of ϱ and an effective mean step separation rather than a single-parameter fit just to ϱ (Ref. 21).
[25] B. Sutherland, J. Math. Phys. **12**, 246 (1971); Phys. Rev. A **4**, 2019 (1971).
[26] Conventionally, the TWD is fit to a Gaussian, from which the variance is gauged via the width at half maximum. This technique provides an adequate approximation if $\tilde{A}$ is not too weak (Ref. 21). However, since Eq. (4) is barely more complicated than a Gaussian, there is little to recommend the Gaussian method (except tradition).
[27] See, e. g., B. Joós, T.L. Einstein, and N.C. Bartelt, Phys. Rev. B **43**, 8153 (1991).
[28] P.J. Forrester, Nucl. Phys. B **388**, 671 (1992); J. Stat. Phys. **72**, 39 (1993).
[29] V.Ya. Krivnov and A.A. Ovchinnikov, Sov. Phys. JETP **55**, 162 (1982).
[30] D. Sen and R.K. Bhaduri, Can. J. Phys. **77**, 327 (1999).
[31] I. S. Gradsteyn and I. M. Ryzhik, *Table of Integrals, Series, and Products* (Academic Press, San Diego, 1980).
[32] See also F. Lesage, V. Pasquier, and D. Serban, Nucl. Phys. B **435[FS]**, 585 (1995). Moreover, Z.N.C. Ha, *ibid.* **435[FS]**, 604 (1995) presents an exact solution for an *arbitrary* value of ϱ. Unfortunately, this solution does not appear to be computationally tractable.
[33] D.M. Gangardt and A. Kamenev, Nucl. Phys. B **610[PM]**, 578 (2001).
[34] For this $\tilde{A}$—in contrast to larger values (Ref. 22) the use of Eq. (4) makes negligible difference from the Gruber-Mullins analysis (Refs. 2,6 and 15) formulated in N.C. Bartelt, T.L. Einstein, and E.D. Williams, Surf. Sci. **240**, L591 (1990).
[35] A. Videcoq, A. Pimpinelli, and M. Vladimirova, Appl. Surf. Sci. **177**, 213 (2001).
[36] M. Degawa, K. Thürmer, I. Morishima, H. Minoda, K. Yagi, and E.D. Williams, Surf. Sci. **487**, 171 (2001), and references therein.
[37] S. Stoyanov, J.J. Métois, and V. Tonchev, Surf. Sci. **465**, 227 (2000).
[38] O. Pierre-Louis and C. Misbah, Phys. Rev. Lett. **76**, 4761 (1996); Phys. Rev. B **58**, 2259 (1998).
[39] E.S. Fu, D.-J. Liu, M.D. Johnson, J.D. Weeks, and E.D. Williams, Surf. Sci. **385**, 259 (1997).
[40] C. Misbah, O. Pierre-Louis, and A. Pimpinelli, Phys. Rev. B **51**, R17 283 (1995).
[41] M. Sato, M. Uwaha, and Y. Saito, Phys. Rev. B **62**, 8452 (2000).
[42] J. Steward, O. Pohland, and J.M. Gibson, Phys. Rev. B **49**, 13 848 (1994).
[43] A. Pimpinelli, V. Tonchev, A. Videcoq, and M. Vladimirova, Phys. Rev. Lett. **88**, 206103 (2002).
[44] More generally, step bunching presumably also involves an altered form of the step-step interaction from an inverse-square dependence on separation. For the point of this simple argument, we ignore this complication.
[45] E.g., P.J. Rous and D.N. Bly, Phys. Rev. B **62**, 8478 (2000).
[46] M. Giesen, Prog. Surf. Sci. **68**, 1 (2001).
[47] M. Giesen, M. Dietterle, D. Stapel, H. Ibach, and D.M. Kolb, Surf. Sci. **384**, 168 (1997).
[48] R. Koch, J.J. Schulz, and K.H. Rieder, Europhys. Lett. **48**, 554 (1999).
[49] Since $\delta(q) = (\epsilon/\pi)(q^2+\epsilon^2)^{-1}, \epsilon \to 0$, the q^{-2} dependence of the offset seems compatible.
[50] A succinct review is T. L. Einstein and S. V. Khare, in *Dynamics of Crystal Surface and Interfaces*, edited by P. M. Duxbury and T. Pence (Plenum, New York, 1997), p. 83.